AIP | Applied Physics Letters

High-frequency nanotube mechanical resonators

J. Chaste, M. Sledzinska, M. Zdrojek, J. Moser, and A. Bachtold

Citation: Appl. Phys. Lett. **99**, 213502 (2011); doi: 10.1063/1.3663630
View online: http://dx.doi.org/10.1063/1.3663630
View Table of Contents: http://apl.aip.org/resource/1/APPLAB/v99/i21
Published by the American Institute of Physics.

Related Articles

Enrichment of live unlabelled cardiomyocytes from heterogeneous cell populations using manipulation of cell settling velocity by magnetic field
Biomicrofluidics 7, 014110 (2013)

Stretching DNA by electric field and flow field in microfluidic devices: An experimental validation to the devices designed with computer simulations
Biomicrofluidics 7, 014109 (2013)

Low-temperature indium-bonded alkali vapor cell for chip-scale atomic clocks
J. Appl. Phys. 113, 064501 (2013)

Multi-layered dielectric cladding plasmonic microdisk resonator filter and coupler
Phys. Plasmas 20, 020701 (2013)

Paper pump for passive and programmable transport
Biomicrofluidics 7, 014107 (2013)

Additional information on Appl. Phys. Lett.

Journal Homepage: http://apl.aip.org/
Journal Information: http://apl.aip.org/about/about_the_journal
Top downloads: http://apl.aip.org/features/most_downloaded
Information for Authors: http://apl.aip.org/authors

ADVERTISEMENT

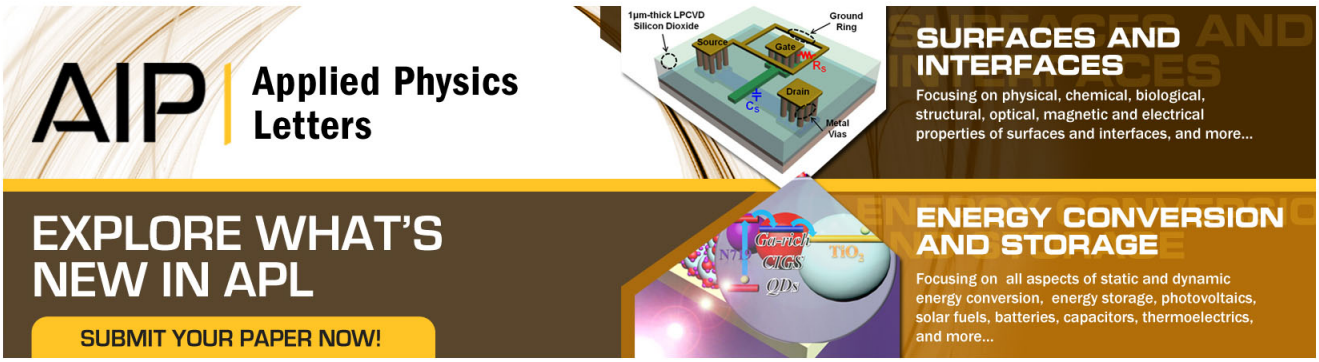

High-frequency nanotube mechanical resonators

J. Chaste, M. Sledzinska, M. Zdrojek, J. Moser, and A. Bachtold[a)]
CIN2(ICN-CSIC), Catalan Institute of Nanotechnology, Campus de la UAB, 08193 Bellaterra (Barcelona), Spain

(Received 30 September 2011; accepted 2 November 2011; published online 21 November 2011)

We report on a simple method to fabricate high-frequency nanotube mechanical resonators reproducibly. We measure resonance frequencies as high as 4.2 GHz for the fundamental eigenmode and 11 GHz for higher order eigenmodes. The high-frequency resonances are achieved using short suspended nanotubes and by introducing tensile stress in the nanotube. These devices allow us to determine the coefficient of the thermal expansion of an individual nanotube, which is negative and is about $-0.7 \cdot 10^{-5}$1/K at room temperature. High-frequency resonators made of nanotubes hold promise for mass sensing and experiments in the quantum limit. © *2011 American Institute of Physics*. [doi:10.1063/1.3663630]

Mechanical resonators have attracted considerable interest as ultra-sensitive detectors of mass[1–5] and force,[6–8] and as macroscopic objects whose motion can be cooled to the quantum limit.[9–11] A key parameter in these experiments is the resonance frequency f_0, which is often desirable to have as high as possible. For instance, a high resonance frequency is expected to improve the sensitivity of mass sensing; it also makes the temperature at which quantum phenomena appear within reach of standard refrigerators. Flexural motion at f_0 higher than 1 GHz was detected using singly and doubly clamped microfabricated resonators.[12,13] Single-wall carbon nanotubes have allowed the fabrication of nanoelectromechanical resonators endowed with excellent properties,[2–5,8,14–20] but the highest reported resonance frequency is rather modest (below 600 MHz).

In this letter, we report on a simple and reliable method to fabricate high-frequency nanotube resonators where f_0 can be as high as 4.2 GHz for the fundamental eigenmode and 11 GHz for higher order eigenmodes. The high-frequency resonators are achieved using a device layout in which the suspended nanotube is short. The resonance frequency is further increased by lowering the temperature T. We attribute the latter behavior to the thermal expansion of the metal electrodes (used to clamp the nanotube), which increases the tensile stress in the nanotube upon lowering T.

Nanotube resonators were fabricated using conventional nanofabrication techniques. Nanotubes were grown by chemical vapor deposition on a highly resistive silicon wafer coated with a 1 μm thick oxide layer. In order to achieve high-frequency resonators, care was taken to (1) design contact electrodes with a short separation ranging from 100 to 700 nm and (2) select straight segments of nanotubes by atomic force microscopy (AFM) to minimize slack once the nanotube is suspended. We used electron-beam lithography and Cr/Au evaporation to pattern contact electrodes as well as a side-gate electrode (Fig. 1(a)). (For those devices whose electrode separation is more than 600 nm, we used a highly doped Si wafer as a backgate.) The nanotubes were suspended by etching ~250 nm of the oxide with fluoridic acid.

Figures 2(a) and 2(b) show two mechanical resonances at 4.2 and 11 GHz for a device whose contact electrodes are ~110 nm apart. The motion was driven and detected using the frequency modulation (FM) mixing technique[18] (Fig. 1(b)). The resonances consist of a central peak flanked by two lobes, which is consistent with the typical lineshape of a mechanical resonance in a FM measurement[18] (the observed asymmetry in the resonances is probably due to the Duffing force). The properties of the resonator slightly changed during the 12 cool-downs experienced by the device. That is, f_0 fluctuated between 3.8 and 4.3 GHz for the lower resonance (f_0 fluctuated between 11 and 11.2 GHz for the higher resonance which we studied in 3 cool-downs only).

These resonances correspond to flexural eigenmodes, since other eigenmodes are expected to have much larger resonance frequencies ($f_0 \approx 240$ GHz for the lowest longitudinal and twisting eigenmodes of a 110 nm long nanotube[21]). We assign the 4.2 GHz resonance to the fundamental eigenmode, since it is the lowest in frequency and shows the largest current signal at resonance. Accordingly, the 11 GHz resonance corresponds to a higher-order eigenmode, which is likely the 3rd mode, since the 2nd mode is expected to be driven weakly due to the symmetry of the device (the gate electrode is symmetrically placed with respect to the nanotube). The ratio between the 11 and the 4.2 GHz frequencies

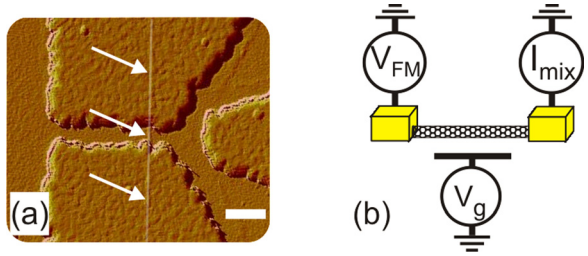

FIG. 1. (Color online) (a) AFM image of the device prior to removal of the supporting oxide. The scale bar is 300 nm. The white arrows point to the nanotube. (b) Schematic of the actuation/detection setup. A frequency modulated voltage V_{FM} is applied to the device. The motion is detected by measuring the mixing current I_{mix}.

[a)]Author to whom correspondence should be addressed. Electronic mail: adrian.bachtold@cin2.es.

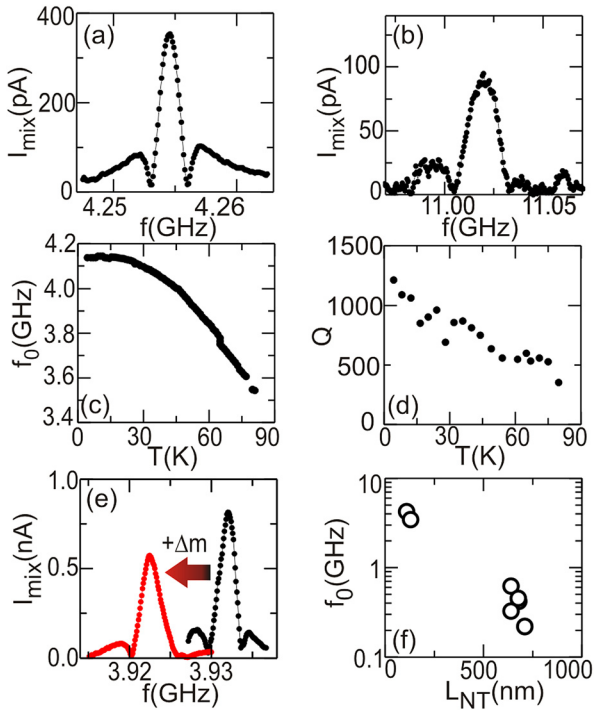

FIG. 2. (Color online) (a) and (b) Mechanical resonances measured at 4 K. The V_{FM} amplitude is 5 mV in (a) and 10 mV in (b). (c) and (d) Temperature dependence of the resonance frequency and of the quality factor for the resonance in (a) measured with $V_{FM}=4$ mV. (e) Frequency shift of the resonance after adding Xe atoms onto the resonator. Xe atoms were admitted in the sample chamber from a gas reservoir at 300 K using a pinhole doser. (f) Resonance frequency as a function of the nanotube length at 4 K for different resonators.

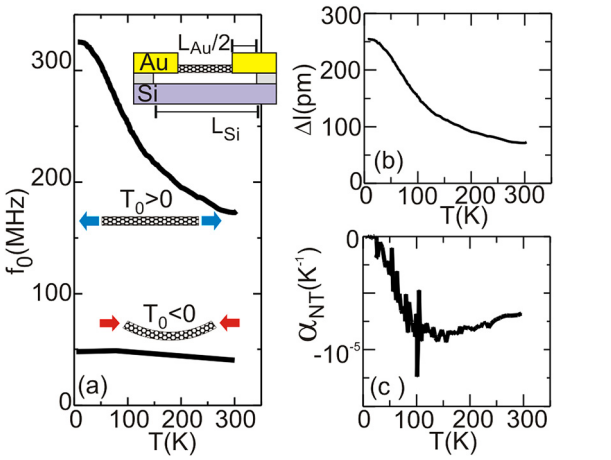

FIG. 3. (Color online) (a)Resonance frequency as a function of T for a 640 nm long nanotube (upper curve, the built-in tension T_0 is positive). For comparison, the lower curve corresponds to the measurement of the lowest resonance of a nanotube with slack ($T_0<0$) whose length is about 1 μm (the device is fabricated as in Ref. 15).The upper inset shows the schematic of the nanotube resonator. (b) Elongation imposed on the nanotube under tensile stress, obtained using $L_{Au}=520$ nm and $L_{Si}=1160$ nm (L_{Au} is taken as twice the etched oxide depth measured with AFM). (c) Thermal expansion coefficient of the nanotube in (b).

is rather close to 3, the value expected for a nanotube under tension. One reason why the ratio is not exactly 3 could be related to the influence of the clamping electrodes.[28]

We confirmed the mechanical origin of these resonances by depositing xenon atoms onto the nanotube *in situ* and observing a drop in the resonance frequencies (Fig. 2(e)). The reason for the drop in f_0 is the adsorption of Xe atoms onto the nanotube surface which increases the mass of the mechanical resonator. Both before and after the adsorption of Xe atoms, the maximum deviation in f_0 was 0.45 MHz (obtained from 22 measurements of the resonance), which is much less than the 10.5 MHz drop in f_0 due to the adsorption of Xe atoms (these results will be further discussed elsewhere). Another signature of the mechanical origin is the strong temperature dependence of f_0 (Fig. 2(c)); we indeed studied dozens of mechanical resonators with the FM mixing technique and occasionally observed some low-amplitude resonances whose origin was purely electrical, but whose f_0 would not change with temperature.

Figure 2(d) shows that the quality factor Q increases upon lowering temperature and reaches 1200 at 4 K and for a driving excitation $V_{FM}=4$ mV. We emphasize that the quality factor varies with the driving excitation (Q increases by a factor $\sim$3 upon increasing V_{FM} from 1 to 10 mV). It is not clear whether this variation is due to nonlinear damping[8,20] or is related to Joule heating (which is induced by the large applied voltage).

Two important parameters that allow us to tune the resonance to high frequency are the length of the suspended nanotube segment (L_{NT}) and the temperature. Indeed, Fig. 2(f) displays the resonance frequency of the fundamental eigenmode at 4 K for the 7 resonators that were fabricated with the method described above; the resonance frequency increases as L_{NT} decreases, as expected for mechanical resonators. In addition, the resonance frequency dramatically increases upon lowering T as shown in Fig. 2(c) and in the upper curve in Fig. 3(a). The latter behavior is related to the T dependence of the tensile stress within the nanotube: in our device layout (inset of Fig. 3(a)), the suspended parts of the clamping Au electrodes contract upon lowering T, thus they increase the tensile stress within the nanotube (the estimated contraction[22] of Au from 300 to 4 K is $|\Delta l_{Au}|\approx 1.6$ nm and is larger than that of Si (Ref. 23) which is $|\Delta l_{Si}|\approx 0.2$ nm in Fig. 3(a)). By contrast, the resonance frequency is weakly sensitive to the voltage applied on the gate (see supplementary information[27]).

From the T dependence of f_0, we evaluate the elongation Δl imposed on the nanotube using the relation

$$f_0 = 0.5\sqrt{T_0/mL_{NT}} \tag{1}$$

valid for a beam under tensile stress and using Hooke's law $\Delta l = T_0 L_{NT}/E\pi(r^2-(r-0.167\,nm)^2)$ for a hollow cylinder with built-in tension T_0. Here $m=2.6$ ag is the mass of the nanotube, $L_{NT}=640$ nm its length, $r=0.85$ nm its radius, and $E=1.25$ TPa its Young's modulus (L_{NT} and r were measured with AFM before the nanotube suspension). Figure 3(b) shows that the elongation and its variation with T are very small (of the order of 100 pm).

We are now in a position to estimate the thermal expansion coefficient (TEC) of an individual nanotube, a property that has not been measured thus far. For this, we use the definition of the TEC

$$\alpha_{NT} = \frac{\Delta l_{NT}}{\Delta T}\frac{1}{L_{NT}} \quad (2)$$

together with the hypothesis of the conservation of length $\Delta l_{NT} = \Delta l_{Si} - \Delta l_{Au} - \Delta l$. Figure 3(c) shows that the TEC of the nanotube is negative and that its magnitude is rather large ($10^{-6} - 10^{-5}$1/K). We obtain similar results for the other nanotubes (for which f_0 could be measured from 300 to 4 K). Interestingly, this TEC is similar to what was recently measured in graphene [24,25] and also to the TEC estimated using numerical simulations on unclamped nanotubes.[26]

In conclusion, we have reported on a simple method to fabricate high-frequency nanotube resonators under tensile stress. The tensile stress increases upon lowering temperature, since the suspended Au electrodes contract. High-frequency resonators made from nanotubes hold promise for various scientific and technological applications, such as mass sensing and experiments in the quantum limit. Finally, our device layout allows us to estimate the TEC of an individual nanotube. In future high-speed, high-density nanotube circuits, a knowledge of the nanotube TEC will help address thermal management issues.

We acknowledge support from the European Union (RODIN, FP7), the Spanish ministry (FIS2009-11284), and the Catalan government (AGAUR, SGR).

[1]Y. T. Yang, C. Callegari, X. L. Feng, K. L. Ekinci, and M. L. Roukes, Nano Lett. **6**, 583 (2006).
[2]B. Lassagne, D. Garcia-Sanchez, A. Aguasca, and A. Bachtold, Nano Lett. **8**, 3735 (2008).
[3]H.-Y. Chiu, P. Hung, H. W. Ch. Postma, and M. Bockrath, Nano Lett. **8**, 4342 (2008).
[4]K. Jensen, K. Kim, and A. Zettl, Nat. Nanotechnol. **3**, 533 (2008).
[5]Z. Wang, J. Wei, P. Morse, J. G. Dash, O. E. Vilches, and D. H. Cobden, Science **327**, 552 (2010).
[6]H. J. Mamin and D. Rugar, Appl. Phys. Lett. **79**, 3358 (2001).
[7]J. D. Teufel, T. Donner, M. A. Castellanos-Beltran, J. W. Harlow, and K. W. Lehnert, Nat. Nanotechnol. **4**, 820 (2009).
[8]A. Eichler, J. Moser, J. Chaste, M. Zdrojek, I. Wilson-Rae, and A. Bachtold, Nat. Nanotechnol. **6**, 339 (2011).
[9]T. Rocheleau, T. Ndukum, C. Macklin, J. B. Hertzberg, A. A. Clerk, and K. C. Schwab, Nature **463**, 72 (2009).
[10]A. D. O'Connell, M. Hofheinz, M. Ansmann, R. C. Bialczak, M. Lenander, E. Lucero, M. Neeley, D. Sank, H. Wang, M. Weides, J. Wenner, J. M. Martinis, and A. N. Cleland, Nature **464**, 697 (2010).
[11]J. D. Teufel, T. Donner, D. Li, J. W. Harlow, M. S. Allman, K. Cicak, A. J. Sirois, J. D. Whittaker, K. W. Lehnert, and R. W. Simmonds, Nature **475**, 359 (2011).
[12]X. M. H. Huang, C. A. Zorman, M. Mehregany, and M. L. Roukes, Nature **421**, 496 (2003).
[13]N. Liu, F. Giesen, M. Belov, J. Losby, J. Moroz, A. E. Fraser, G. McKinnon, T. J. Clement, V. Sauer, W. K. Hiebert, and M. R. Freeman, Nat. Nanotechnol. **3**, 715 (2008).
[14]V. Sazonova, Y. Yaish, H. Üstünel, D. Roundy, T. A. Arias, and P. L. McEuen, Nature **431**, 284 (2004).
[15]A. K. Hüttel, G. A. Steele, B. Witkamp, M. Poot, L. P. Kouwenhoven, and H. S. J. van der Zant, Nano Lett. **9**, 2547 (2009).
[16]B. Lassagne, Y. Tarakanov, J. Kinaret, D. Garcia-Sanchez, and A. Bachtold, Science **325**, 1107 (2009).
[17]G. A. Steele, A. K. Hüttel, B. Witkamp, M. Poot, H. B. Meerwaldt, L. P. Kouwenhoven, and H. S. J. van der Zant, Science **325**, 1103 (2009).
[18]V. Gouttenoire, T. Barois, S. Perisanu, J.-L. Leclercq, S. T. Purcell, P. Vincent, and A. Ayari, Small **6**, 1060 (2010).
[19]C. C. Wu and Z. Zhong, Nano Lett. **11**, 1448 (2011).
[20]A. Eichler, J. Chaste, J. Moser, and A. Bachtold, Nano Lett. **11**, 2699 (2011).
[21]S. Sapmaz, P. Jarillo-Herrero, Y. M. Blanter, C. Dekker, and H. S. J. van der Zant, Phys. Rev. Lett. **96**, 026801 (2006).
[22]J. F. C. Nix and D. MacNair, Phys. Rev. **60**, 597 (1940).
[23]K. G. Lyon, G. L. Salinger, C. S. Swenson, and G. K. White, J. Appl. Phys. **48**, 865 (1977).
[24]W. Bao, F. Miao, Z. Chen, H. Zhang, W. Jang, C. Dames, and C. N. Lau, Nat. Nanotechnol. **4**, 562 (2009).
[25]V. Singh, S. Sengupta, H. S. Solanki, R. Dhall, A. Allain, S. Dhara, P. Pant, and M. Deshmukh, Nanotechnology **21**, 165204 (2010).
[26]Y. K. Kwon, S. Berber, and D. Tománek, Phys. Rev. Lett. **92**, 015901 (2004).
[27]See supplementary material at http://dx.doi.org/10.1063/1.3663630 for the gate voltage dependence of the resonance frequency for the nanotube under tensile stress and the nanotube with slack in Fig. 3(a).
[28]I. Wilson-Rae, private communication (2010).